CHAPTER 2

A NOVEL TORQUE CONTROL STRATEGY FOR IPMSM DRIVES

2.1 Introduction

Due to the merits of being able to achieve higher efficiency, higher power density, higher torque to inertia ratio and free from maintenance, permanent magnet synchronous motors (PMSM) are now receiving growing research interests in many industrial drive applications such as in air conditioner drives [1, 2], hybrid and fuel cell vehicle drives [3] as well as traction and machine tool spindle drives [5]. In particular, if the permanent magnets are buried inside the rotor core, the resulting PMSM, called interior permanent magnet synchronous motor (IPMSM), has a mechanically robust rotor structure that is very suitable for high speed operation. Moreover, due to the difference between the d- and q-axis inductances, the IPMSM possesses an extra torque component, namely the reluctance torque, as compared with that of a surface mounted PMSM.

Basically, there are two types of torque controller for IPMSM in existing literature. The first type [e.g. 8-10], can be classified as a linear torque controller that keeps zero d-axis stator current (i_{ds}) such that the resulting electromagnetic torque is proportional to the q-axis stator current (i_{qs}). This will, of course, make the controller design much easier. However, the reluctance torque of the IPMSM is not fully exploited. The second class, namely nonlinear torque controller where the resulting torque contains a nonlinear term $i_{ds}\, i_{qs}$, however, takes advantage of the reluctance torque. For example, this class includes the unity power factor control [11], constant stator flux linkage control [11], maximum torque per

ampere (MTPA) control [12-16], and maximum efficiency control [17, 18]. In view of the above classification, the question is that whether it is possible to have a linear torque controller that can also fully exploit the reluctance torque to achieve higher output power capability. The answer of this question is yes and is, in fact, the main contribution of this chapter.

The rest of this chapter may be outlined as follows. In section 2.2, the mathematical model of the IPMSM is first reviewed briefly. Then, the torque constant of the proposed torque control strategy is optimized in Section 2.3. An implementation example of the proposed torque controller is then presented in Section 2.4. Also, some experimental results are given for illustrating the feasibility of the proposed torque control strategy.

2.2 Mathematical Model of an IPMSM

For convenience, the dynamic model of an IPMSM in the rotor reference frame will be repeated [64] as follows

$$v_{ds} = \mathrm{R_S}\, i_{ds} + \frac{d\lambda_{ds}}{dt} - \omega_r \mathrm{L_q}\, i_{qs} \tag{2.1}$$

$$v_{qs} = \mathrm{R_S}\, i_{qs} + \frac{d\lambda_{qs}}{dt} + \omega_r\, (\mathrm{L_d}\, i_{ds} + \lambda_{\mathrm{mf}}) \tag{2.2}$$

$$\lambda_{ds} = \mathrm{L_d}\, i_{ds} + \lambda_{\mathrm{mf}} \tag{2.3}$$

$$\lambda_{qs} = \mathrm{L_q}\, i_{qs} \tag{2.4}$$

$$T_{\mathrm{e}} = \frac{3}{2}\frac{\mathrm{p}}{2} \left[\lambda_{\mathrm{mf}} + (\mathrm{L_d}\text{-}\mathrm{L_q})\, i_{ds} \right] i_{qs} \tag{2.5}$$

where

v_{ds}, v_{qs} : stator d-axis and q-axis voltages

i_{ds}, i_{qs} : stator d-axis and q-axis currents

$\mathrm{R_S}$: stator winding resistance

L_d, L_q : stator d-axis and q-axis inductances

λ_{ds}, λ_{qs} : stator d-axis and q-axis flux linkages

λ_{mf} : rotor permanent magnet flux linkage

ω_r : electrical angular frequency

p : number of poles

T_e : generated torque of an IPMSM

The corresponding d- and q-axis dynamic equivalent circuits of an IPMSM in the rotor reference frame are given in Fig. 2.1. Since under steady state, λ_{ds} and λ_{qs} become constants and equations (2.1) and (2.2) reduce to the following form

$$v_{ds} = R_S i_{ds} - \omega_r L_q i_{qs} \tag{2.6}$$

$$v_{qs} = R_S i_{qs} + \omega_r (L_d i_{ds} + \lambda_{mf}) \tag{2.7}$$

From (2.5) one can see that when i_{ds} is equal to zero, then

$$T_e = \frac{3}{2}\frac{p}{2}\lambda_{mf} i_{qs} \tag{2.8}$$

It is seen from (2.8) that the resulting torque is proportional to i_{qs}. Hence, it is quite straightforward to implement a vector controller [8-10] to achieve high performance. However, in case i_{ds} is not equal to zero, then from (2.5) one can see that T_e will contain a nonlinear term, namely $i_{ds} i_{qs}$. Thus, the question is "Does a linear torque control (LTC)

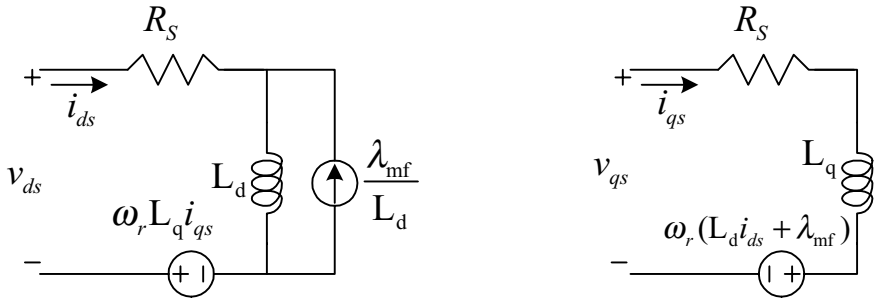

Fig. 2.1. The d- and q-axis dynamic equivalent circuits of an IPMSM in the rotor reference frame.

strategy with $i_{ds} \neq 0$ exist?" Intuitively, one may pose the following form for the above problem:

$$T_e = C\ \mathrm{sgn}(i_{qs})\left|\vec{i}_s\right| \tag{2.9}$$

where

$$\begin{aligned}\vec{i}_s &\triangleq i_{ds} + j\ i_{qs} \\ &= \frac{2}{3}(i_{as} + a\ i_{bs} + a^2\ i_{cs})\end{aligned} \tag{2.10}$$

$$\left|\vec{i}_s\right| \triangleq \sqrt{i_{ds}^2 + i_{qs}^2} \tag{2.11}$$

$$a \triangleq e^{j(2/3)\pi}$$

$\mathrm{sgn}(i_{qs})$ means the sign of i_{qs} and C is a positive constant. From (2.9) one can see that if $i_{ds} = 0$ then it just reduces to the familiar linear form of $T_e = C\, i_{qs}$. Also, inclusion of $\mathrm{sgn}(i_{qs})$ in (2.9) is to take care of the deceleration case with negative torque.

2.3 Optimization of the Torque Constant

Suppose that the linear torque control relation of (2.9) does exist. Then, it is naturally desired to maximize the torque constant. First, define the following constant

$$m \triangleq \frac{C}{\frac{3}{2}\frac{p}{2}\lambda_{mf}} \tag{2.12}$$

It follows from (2.5) and (2.9) that

$$m = \frac{1 + \frac{(L_d - L_q)}{\lambda_{mf}} i_{ds}}{(1 + \frac{i_{ds}^2}{i_{qs}^2})^{0.5}} \tag{2.13}$$

To fully exploit the reluctance torque, the stator d-axis current (i_{ds}) should be less than or equal to zero. It follows from (2.13) and the fact of $L_d - L_q < 0$ for IPMSM that m is greater than zero. Hence, one may maximize m^2 as well to achieve the optimal C value. Hence, from (2.13) one has

$$\frac{\partial m^2}{\partial i_{qs}}\Big|_{i_{ds}=const.} = \frac{2i_{ds}^2 |i_{qs}|}{(i_{ds}^2 + i_{qs}^2)^2}\left[1 + \frac{2(L_d - L_q)i_{ds}}{\lambda_{mf}} + \frac{(L_d - L_q)^2}{\lambda_{mf}^2} i_{ds}^2\right] \tag{2.14}$$

From (2.14) one can see that in case $i_{ds} = 0$, then (2.14) also becomes zero and $m = 1$. On the other hand, when $i_{ds} < 0$ then (2.14) is always positive as far as the IPMSM characteristic is concerned. This fact indicates that, for each i_{ds}, m^2 is a monotonically increasing function with respect to i_{qs}. Thus, existence of the proposition of the linear form of (2.9) can now be guaranteed by the following condition:

$$m^2 \geq 1 \tag{2.15}$$

or equivalently

$$i_{ds}\left[(L_d - L_q)^2 i_{qs}^2 - \lambda_{mf}^2\right] \leq -2\lambda_{mf}(L_d - L_q)i_{qs}^2 \tag{2.16}$$

Since as far as a practical IPMSM is concerned,

$$(L_d - L_q)^2 i_{qs}^2 - \lambda_{mf}^2 < 0, \tag{2.17}$$

it follows from (2.16) that

$$i_{ds} \geq \frac{-2\lambda_{mf}(L_d - L_q)i_{qs}^2}{(L_d - L_q)^2 i_{qs}^2 - \lambda_{mf}^2} \tag{2.18}$$

In view of the above results, one can observe that it is indeed possible to get a linear torque control relation as (2.9) where

$$C=\frac{3}{2}\frac{p}{2}\lambda_{mf} \quad , \tag{2.19}$$

is obtained for m=1 and

$$i_{ds}=\frac{-2\lambda_{mf}(L_d-L_q)i_{qs}^2}{(L_d-L_q)^2\ i_{qs}^2-\lambda_{mf}^2} \tag{2.20}$$

In other words, so long as (2.19) and (2.20) are satisfied, then the resulting torque T_e will be proportional to the magnitude of the stator line current whenever inequality (2.18) and $i_{ds} \le 0$ are satisfied. Thus, not only the existence condition of the previously posed question is obtained but also the closed form relation between i_{ds} and i_{qs} is achieved. For practical inverter-fed drives, there also exist output voltage and output current constraints. Assume that the maximum phase voltage magnitude and line current magnitude are V_{sm} and I_{sm} respectively. Then the feasible range of i_{ds} for (2.20) can be decided by considering the following constraints

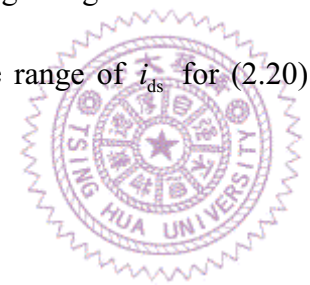

$$i_{ds}^2+i_{qs}^2 \le I_{sm}^2 \tag{2.21}$$

$$v_{ds}^2+v_{qs}^2 \le V_{sm}^2 \tag{2.22}$$

Thus, the boundary of the linear torque region, namely i_{dsm} can be determined by substituting $i_{qs}=\sqrt{I_{sm}^2-i_{dsm}^2}$ into (2.20) yielding

$$\begin{aligned}&(L_d-L_q)^2\ i_{dsm}^3+2\lambda_{mf}\ (L_d-L_q)\ i_{dsm}^2+\\&[\lambda_{mf}^2-(L_d-L_q)^2\ I_{sm}^2]\ i_{dsm}-2\lambda_{mf}(L_d-L_q)I_{sm}^2=0\end{aligned} \tag{2.23}$$

Meanwhile the maximum angular speed, namely ω_{rm}, to maintain the maximum torque $T_{em}=\frac{3}{2}\frac{p}{2}\ \lambda_{mf}\ I_{sm}$ can be calculated from the following equation

$$V_{sm}^2 = (R_s i_{dsm} - \omega_{rm} L_q i_{qsm})^2 + \left[R_s i_{qsm} + \omega_{rm} (L_d i_{dsm} + \lambda_{mf}) \right]^2 \quad (2.24)$$

where equations (2.6) and (2.7) have been applied in the derivation of (2.24) and $i_{qsm} = \sqrt{I_{sm}^2 - i_{dsm}^2}$.

In order to facilitate understanding the significance of the proposed torque control strategy, three sets of IPMSM drive parameters from [13, 51, and 65] are selected as examples. Table 2.1 shows the corresponding parameter values of these IPMSMs. For later experiment, parameters of motor D that was designed in [67] are also listed on the same table. Fig. 2.2 shows the corresponding maximum torque-speed characteristics for the three motors. For comparison, Table 2.2 also summarizes some important data for three motor drives of Table 2.1. From Fig. 2.2 one can see that for A motor, the constant torque region can be extended to 197 % of that of $i_{ds} = 0$ control strategy. Similarly, for motors B and C, one can increase the constant torque region up to 167 % and 142 % as compared with that of the $i_{ds} = 0$ control strategy.

Table 2.1. IPMSM parameters and some inverter ratings.

IPMSM / parameters	A[ref.13]	B[ref.51]	C[ref.65]	D
number of poles	4	4	4	6
armature resistance(Ω)	0.57	4.30	1.93	0.15
d-axis inductance (mH)	8.72	27.00	42.44	0.488
q-axis inductance (mH)	22.8	67.0	79.57	1.01
magnetic flux linkage (V/(rad/sec))	0.0882	0.272	0.314	0.042
maximum phase voltage magnitude (V)	41	173	170	50
maximum phase current magnitude (A)	7.07	6.0	4.24	25.0

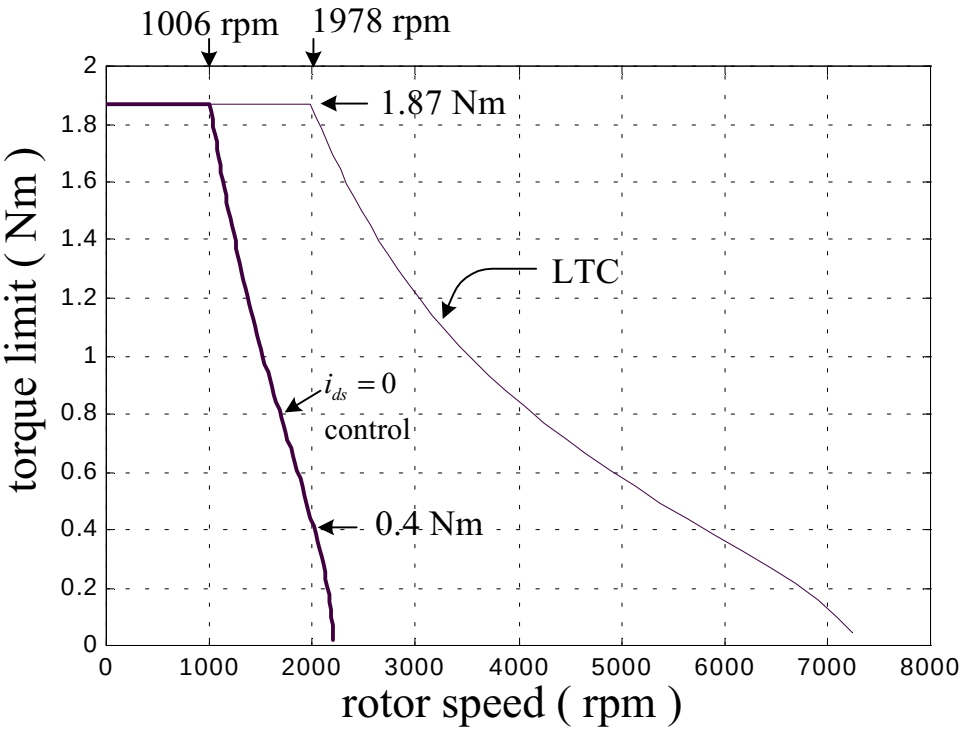

(a)IPMSM A of Table 2.1.

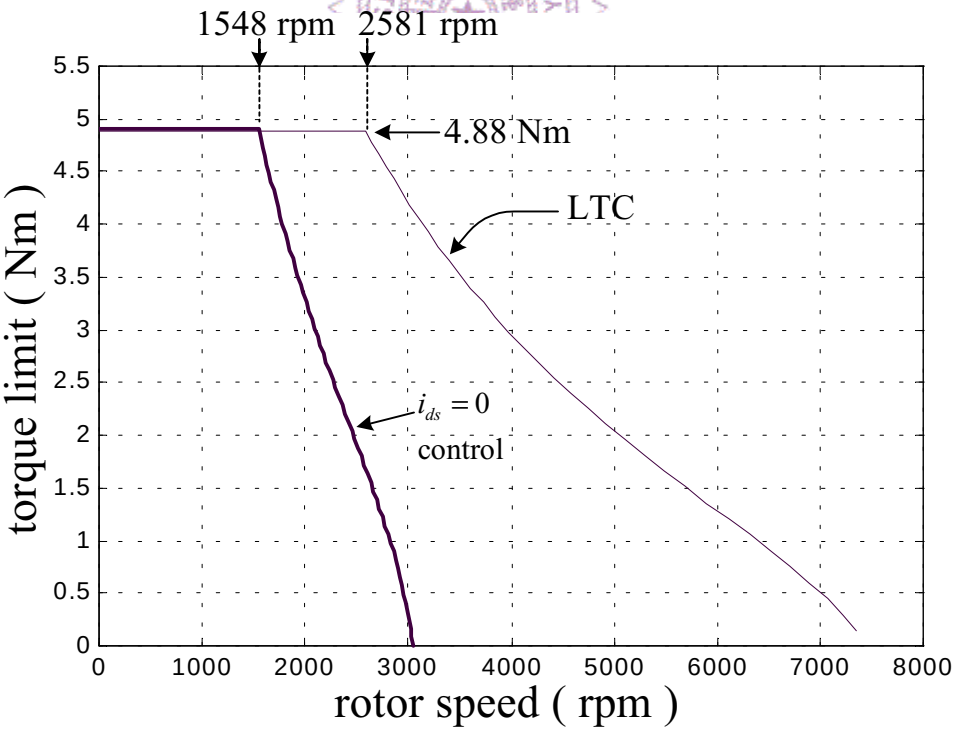

(b) IPMSM B of Table 2.1.

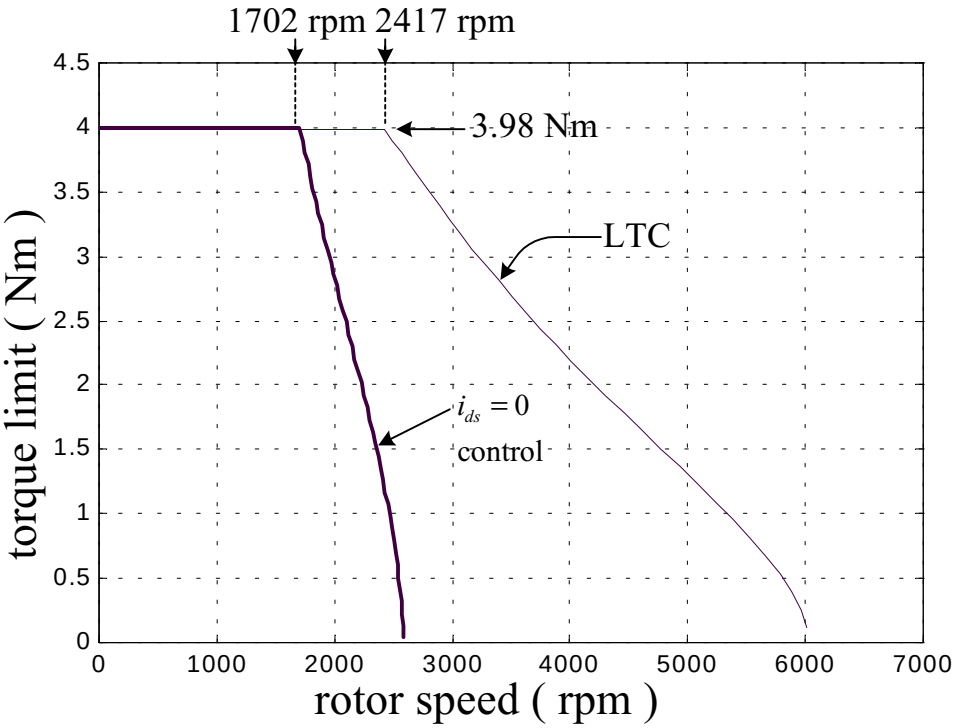

(c) IPMSM C of Table 2.1.

Fig. 2.2. The maximum torque limit to speed profiles for $i_{ds}=0$ control and the proposed LTC for three different IPMSMs.

Table 2.2. Summary of some important data for three motor drives of Table 2.1.

IPMSM	A[ref. 13]				B[ref. 51]				C[ref. 65]			
variables / control strategies	i_{dsm} (A)	T_{em} (Nm)	ω_{rm} (rpm)	$\frac{\omega_{rm}(1)}{\omega_{rm}(2)}$	i_{dsm} (A)	T_{em} (Nm)	ω_{rm} (rpm)	$\frac{\omega_{rm}(1)}{\omega_{rm}(2)}$	i_{dsm} (A)	T_{em} (Nm)	ω_{rm} (rpm)	$\frac{\omega_{rm}(1)}{\omega_{rm}(2)}$
the proposed LTC (1)	-6.08	1.87	1978	197%	-4.86	4.88	2581	167%	-2.79	3.98	2417	142%
$i_{ds}=0$ control (2)	0	1.87	1006		0	4.88	1548		0	3.98	1702	

Furthermore, consider Fig. 2.2(a) as an illustration of the merit of using the proposed torque control strategy. In case the IPMSM is running at 1978 rpm, one can see that the maximum torque (1.87 Nm) can still be obtained. However, if the control strategy of $i_{ds} = 0$ is adopted, then the corresponding available torque is only 0.4 Nm approximately. In other words, the proposed torque control strategy can provide more output power and better performance at higher speed range as compared with that of $i_{ds} = 0$ control. Finally, it should be mentioned that if $\omega_r > \omega_{rm}$, then the motor torque will be reduced also for the proposed strategy. Therefore, the corresponding field weakening control will be presented in the next chapter.

2.4 Implementation of the Proposed Linear Torque Control Strategy

In order to check the validity of the proposed torque control strategy, a prototype is constructed for experiment. The tested IPMSM, a prototype designed in [67], has the parameters of motor D as shown in Table 2.1. Fig. 2.3 also shows the characteristic curve of the proposed torque control strategy on the i_{ds}-i_{qs} plane. The current limit trajectory as well as two voltage limit trajectories, corresponding to ω_r =3500 rpm and 3050 rpm, respectively are also imposed on the same figure for reference. From Fig. 2.3 one can see that the constant torque operation region is bounded by $-12.4(\text{A}) = i_{dsm} \le i_{ds} \le 0$. Also, the corresponding maximum speed (ω_{rm}) for constant torque control is equal to 3500 rpm approximately. In order to simplify the calculations of finding i_{ds}^* and i_{qs}^* for a given line current magnitude $\left|\vec{i}_s^*\right|$, one can substitute $i_{qs} = \sqrt{\left|\vec{i}_s^*\right|^2 - i_{ds}^{*\,2}}$ into (2.20) to get

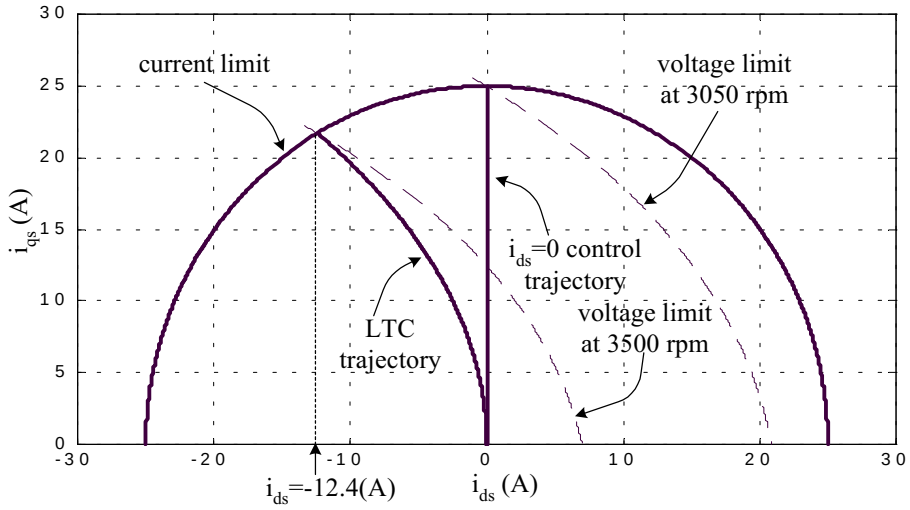

Fig. 2.3. Trajectories of the proposed LTC and $i_{ds}=0$ control as well as the voltage and current limits on i_{ds}-i_{qs} plane for the tested IPMSM.

$$(\mathrm{L_d}\text{-}\mathrm{L_q})^2\ i_{ds}^{*\,3}+2\lambda_{\mathrm{mf}}\ (\mathrm{L_d}\text{-}\mathrm{L_q})\ i_{ds}^{*\,2}+$$

$$[\lambda_{\mathrm{mf}}^2-(\mathrm{L_d}\text{-}\mathrm{L_q})^2\ \left|\vec{i}_s^{\,*}\right|^2]\ i_{ds}^{*}-2\lambda_{\mathrm{mf}}(\mathrm{L_d}\text{-}\mathrm{L_q})\left|\vec{i}_s^{\,*}\right|^2=0 \tag{2.25}$$

and substitute $i_{ds}=-\sqrt{\left|\vec{i}_s^{\,*}\right|^2-i_{qs}^{*\,2}}$ into (2.20) to obtain

$$(\mathrm{L_d}\text{-}\mathrm{L_q})^4\ i_{qs}^{*\,6}+\left[2\lambda_{\mathrm{mf}}^2(\mathrm{L_d}\text{-}\mathrm{L_q})^2-(\mathrm{L_d}\text{-}\mathrm{L_q})^4\left|\vec{i}_s^{\,*}\right|^2\right]\ i_{qs}^{*\,4}+$$

$$[2\lambda_{\mathrm{mf}}^2(\mathrm{L_d}\text{-}\mathrm{L_q})^2\left|\vec{i}_s^{\,*}\right|^2+\lambda_{\mathrm{mf}}^4]\ i_{qs}^{*\,2}-\lambda_{\mathrm{mf}}^4\left|\vec{i}_s^{\,*}\right|^2=0 \tag{2.26}$$

Hence, from (2.25) and (2.26) one can use a second order polynomial to approximate the corresponding i_{ds}^{*} and i_{qs}^{*}, respectively as follows

$$i_{ds}^{*}=a\left|\vec{i}_s^{\,*}\right|^2+b\left|\vec{i}_s^{\,*}\right|+c \tag{2.27}$$

$$i_{qs}^{*}=d\left|\vec{i}_s^{\,*}\right|^2+e\left|\vec{i}_s^{\,*}\right|+f \tag{2.28}$$

From actual experiments, the coefficients a, b, and c in (2.27) are –0.016911, -0.089245, and 0.19176 respectively and the coefficients d, e, and f in (2.28) are –0.0071927, 1.05459, and –0.093642 respectively corresponding to the tested IPMSM. It is found that the

maximum d-axis current error is about 0.2A which is 0.8% of the maximum line current limit (25A) and the maximum q-axis current error is about 0.1A which is 0.4% of the same maximum line current limit. Thus, a second order polynomial approximation is reasonable for the test. Then the numerical calculations can be simplified greatly. Fig. 2.4 shows the block diagram of an implementation of the proposed torque control strategy by using a fixed point DSP TMS320F240. From Fig. 2.4 one can see that a digital PI speed controller is used to generate the desired line current magnitude command, $\pm\left|\vec{i}_s^{\,*}\right|$ which is of course proportional to the desired torque command for the proposed torque control strategy.

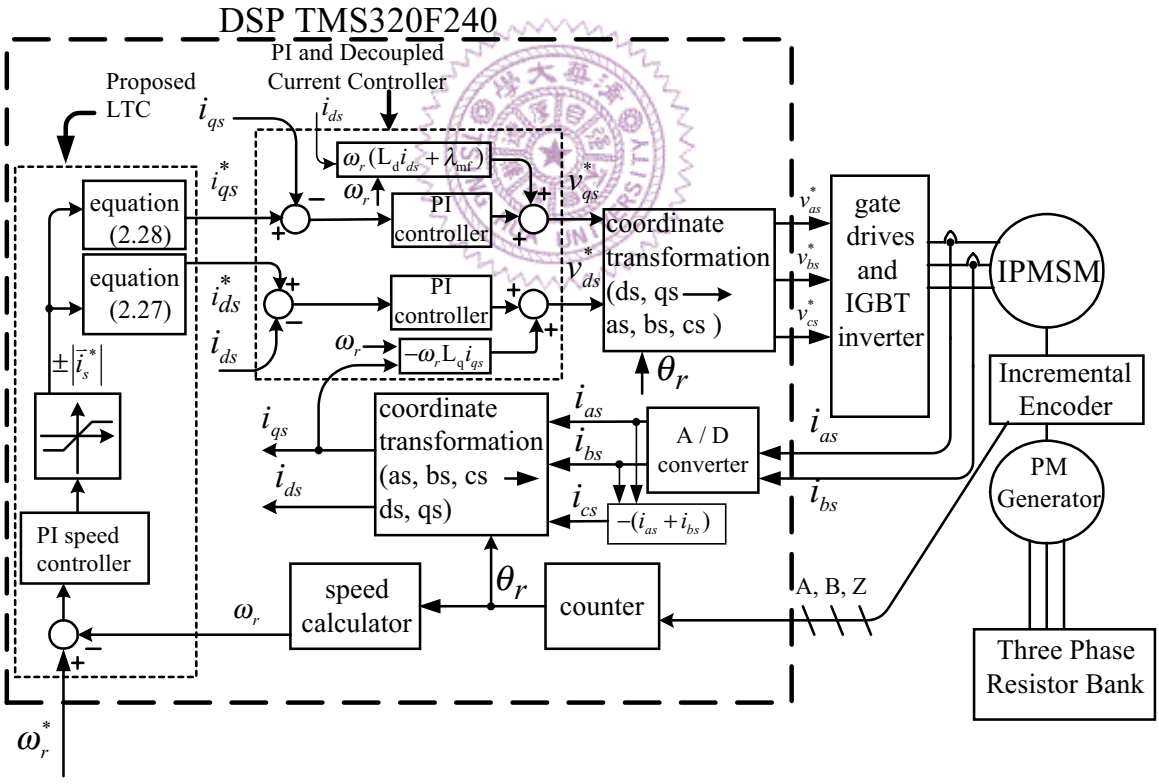

Fig. 2.4. An implementation block diagram of the proposed LTC strategy

The resulting $\pm\left|\vec{i}_s^*\right|$ command is then used to generate the i_{ds}^* and i_{qs}^* by using (2.27) and (2.28) respectively. The sampling time period for this speed loop is chosen to be 1 msec. Similarly, two digital PI controllers are used to generate the desired v_{ds}^* and v_{qs}^* commands. To achieve fast response, decoupling controls [64] are also added to each PI controller to cancel the cross coupling effects between d-axis and q-axis. The sampling time period of this current loop is chosen to be 0.1 msec. The remaining parts of Fig. 2.4 are quite typical and will not be explained further.

To demonstrate the merits of the proposed torque control strategy, first consider the case of applying a step command of $\omega_r = \omega_{rm}$ =3500 rpm to the tested IPMSM drive starting from rest at t=0 sec and with no load. Then, at t=2.2 sec, a step load of 3.4 Nm is added. Figs. 2.4 and 2.5 show the experimental results for the $i_{ds} = 0$ control and the proposed linear torque control, respectively. Except the i_{ds} and i_{qs} component distribution, all other parameters are kept the same for both control strategies. Since the command of 3500 rpm is greater than the maximum angular velocity ω_{rm} =3050 rpm for the $i_{ds} = 0$ control, one can see from Fig. 2.4 that a steady state speed error exists for this high speed command. However, as can be observed from Fig. 2.6, using the proposed torque control strategy can eliminate the steady state speed error. Also from Fig. 2.6, it is seen that i_{ds} is negative and hence the reluctance torque is indeed taken advantage of. As another example, consider the second case of applying a step command of 3500 rpm to the same tested motor drive starting also from rest but with a y-connected resistance load (21 Ω for each phase) connected at the output terminal of the coupled PM generator. Under steady state, the corresponding torque is approximately 3.4 Nm. Figs. 2.6 and 2.7 show the corresponding experimental results for

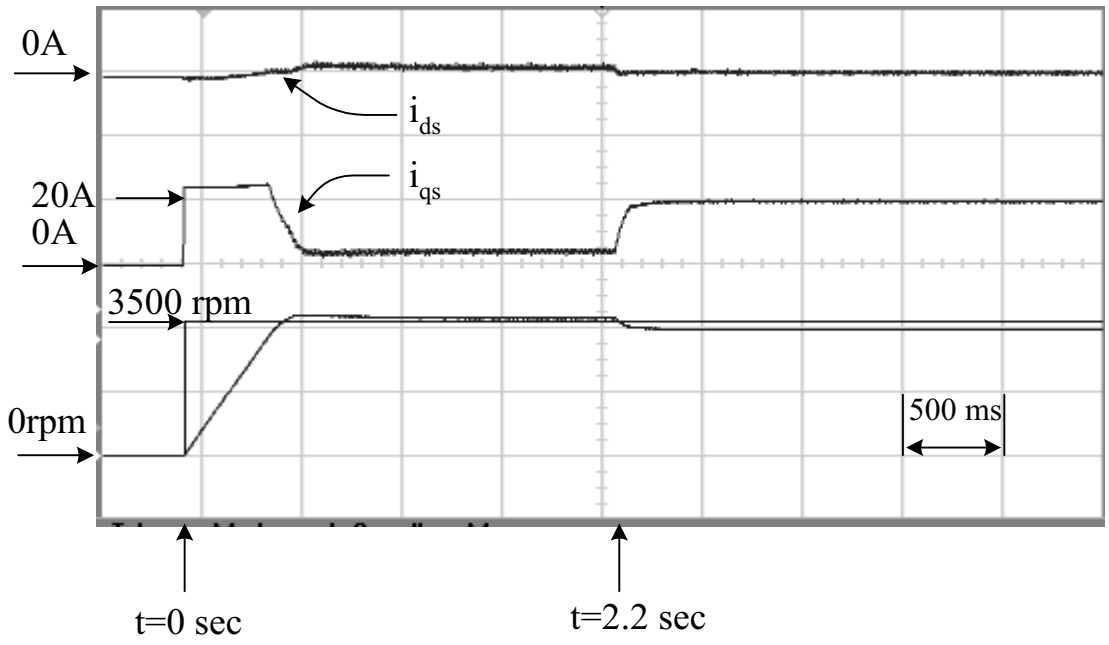

Fig. 2.4. Experimental results of i_{ds}, i_{qs}, and the speed responses for $i_{ds}=0$ control.

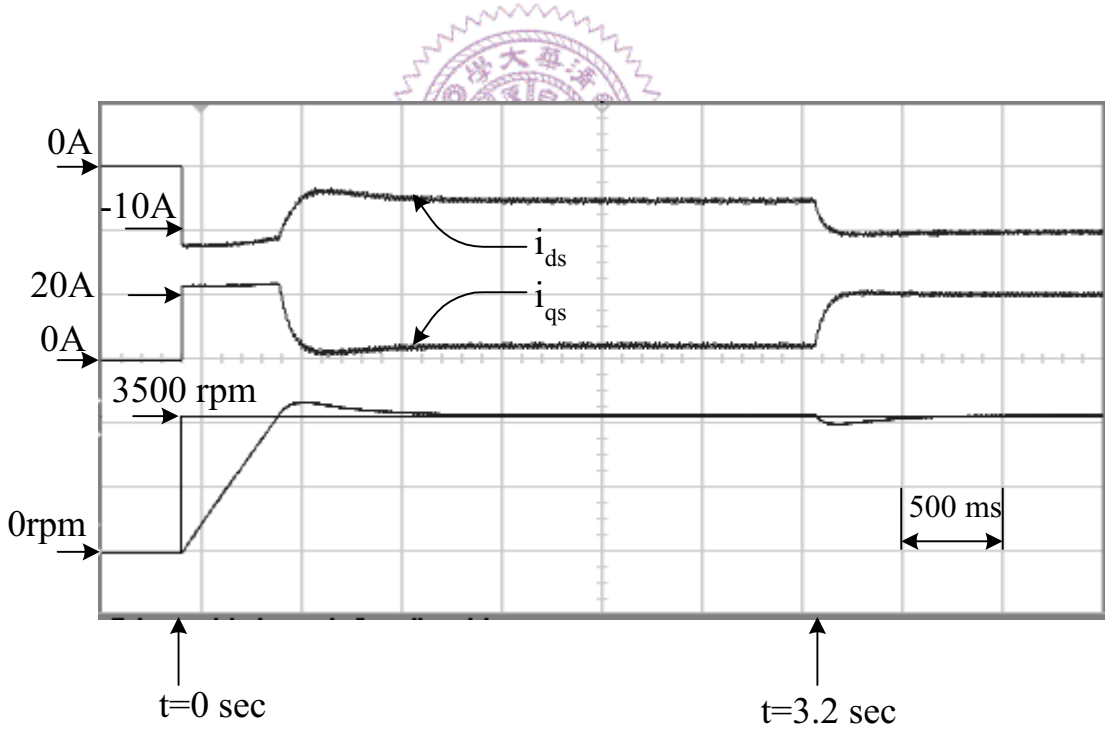

Fig. 2.6. Experimental results of i_{ds}, i_{qs}, and the speed responses for the proposed LTC.

$i_{ds} = 0$ control as well as for the proposed linear torque control. As long as the rotor speed is within the constant torque region, the speed responses for both control strategies agree each other rather closely. This is because of the fact that the same T_{em} is applied. However, as ω_r is increased beyond 3050 rpm, the control strategy with $i_{ds} = 0$ can not supply enough torque to the load. Hence, the final speed settles down at 3214 rpm as shown in Fig. 2.7. With the proposed linear torque control, the drive can still be operated within the constant torque region. Thus, the command can be followed without steady state error as can be seen from Fig. 2.8. For references, Figs. 2.8 and 2.9 also show the corresponding phase-a current for both control strategies respectively. Again, one can see from Fig. 2.9 that the steady state line current for the $i_{ds} = 0$ control is about 20 A and a steady state speed error exists. However, for the proposed torque control, the corresponding line current is about 23 A and no steady state speed error exists as can be seen from Fig. 2.10.

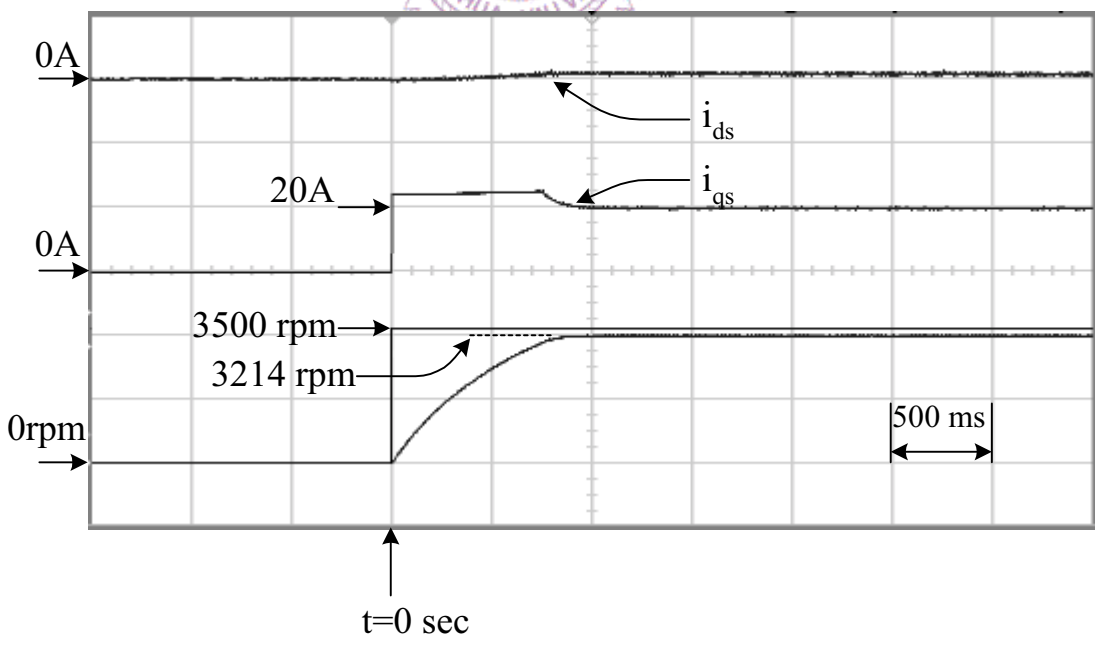

Fig. 2.7. Experimental results of i_{ds}, i_{qs}, and the speed responses for $i_{ds} = 0$ control.

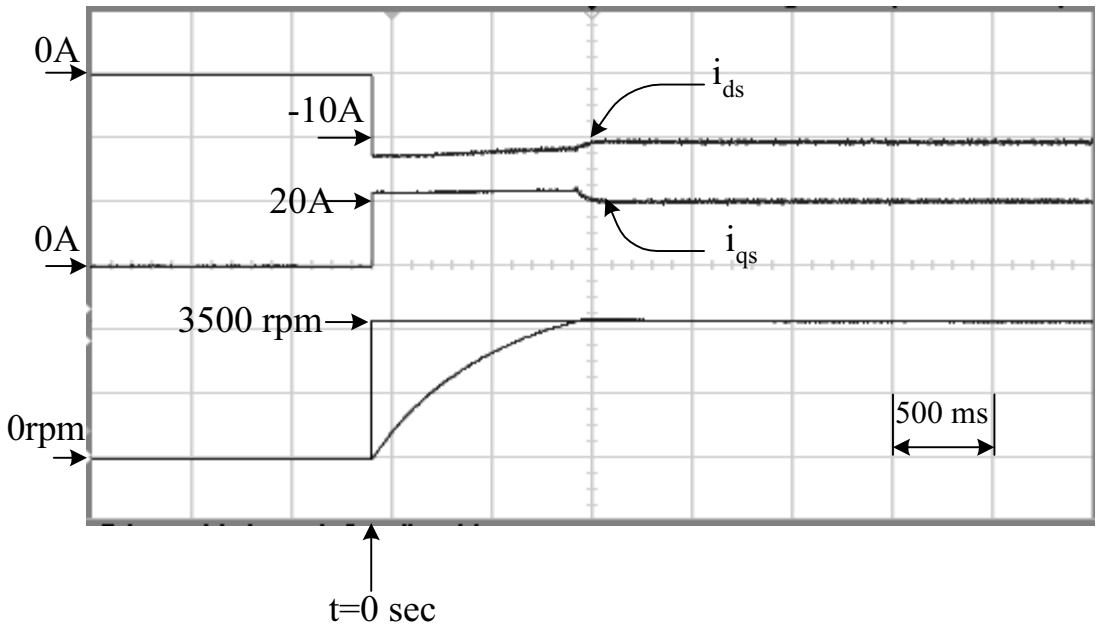

Fig. 2.8. Experimental results of i_{ds}, i_{qs}, and the speed responses for the proposed LTC.

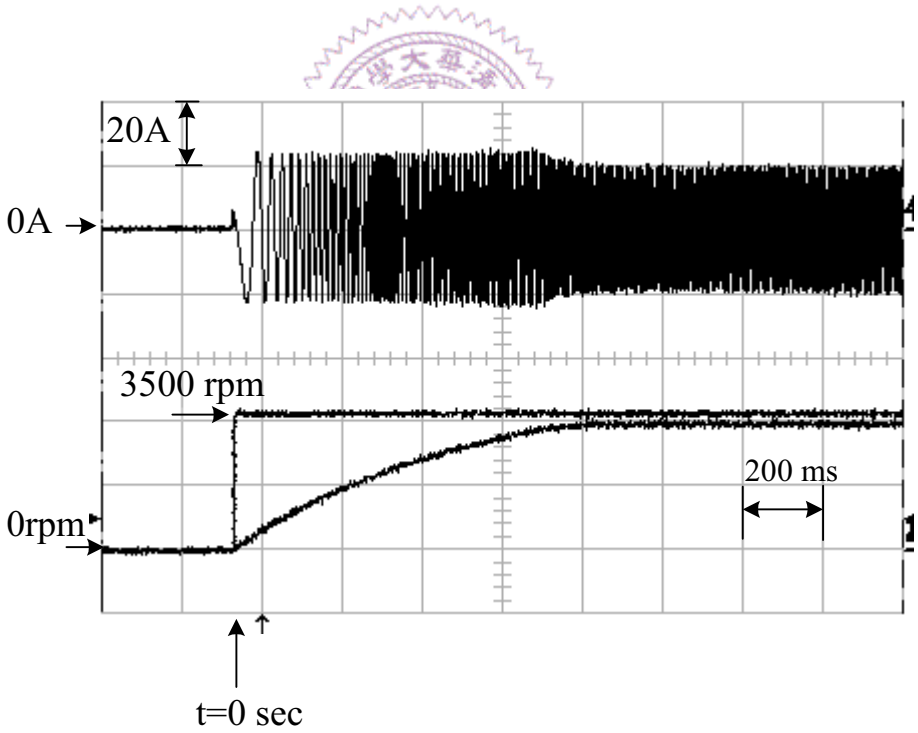

Fig. 2.9. Experimental results of phase-a current and the speed responses corresponding to Fig. 2.7.

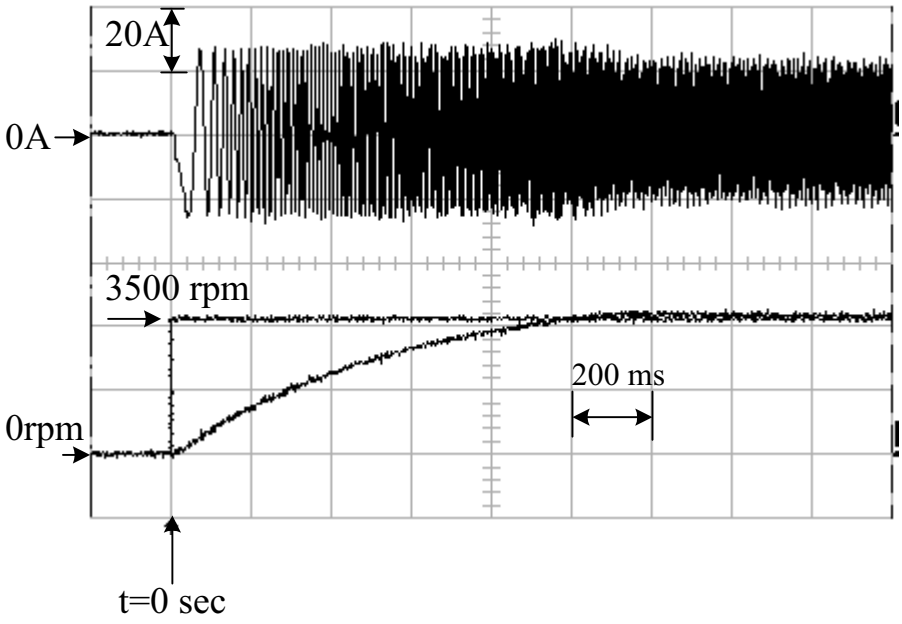

Fig. 2.10. Experimental results of phase-a current and the speed responses corresponding to Fig. 2.8.